

PAPER • OPEN ACCESS

Stretchable inkjet-printed electronics on mechanically compliant island-bridge architectures covalently bonded to elastomeric substrates

To cite this article: Manuel Pietsch *et al* 2022 *Flex. Print. Electron.* 7 025007

View the [article online](#) for updates and enhancements.

You may also like

- [All-in-one electrochromic transparency-tuning window with an integrated metal-mesh heating film](#)
Wenjing He, Chenchao Huang, Xinzhou Wu et al.
- [Aliphatic and aromatic amine based nitrogen-doped carbon dots: a comparative photophysical study](#)
Leepsa Mishra, Ranjan Kumar Behera, Aradhana Panigrahi et al.
- [TiO₂ nanowires for potential facile integration of solar cells and electrochromic devices](#)
Pengfei Qiang, Zhongwei Chen, Peihua Yang et al.



IOP | ebooks™

Bringing together innovative digital publishing with leading authors from the global scientific community.

Start exploring the collection—download the first chapter of every title for free.

Flexible and Printed Electronics



PAPER

OPEN ACCESS

RECEIVED
14 March 2022

REVISED
20 April 2022

ACCEPTED FOR PUBLICATION
3 May 2022

PUBLISHED
13 May 2022

Original content from this work may be used under the terms of the [Creative Commons Attribution 4.0 licence](https://creativecommons.org/licenses/by/4.0/).

Any further distribution of this work must maintain attribution to the author(s) and the title of the work, journal citation and DOI.



Stretchable inkjet-printed electronics on mechanically compliant island-bridge architectures covalently bonded to elastomeric substrates

Manuel Pietsch^{1,2}, Stefan Schliske^{1,2}, Martin Held^{1,2}, Patrick Maag^{1,2} and Gerardo Hernandez-Sosa^{1,2,3,*}

¹ Light Technology Institute, Karlsruhe Institute of Technology, Engesserstr. 13, 76131 Karlsruhe, Germany

² InnovationLab, Speyererstr. 4, 69115 Heidelberg, Germany

³ Institute of Microstructure Technology, Hermann-von-Helmholtz-Platz 1, 76344 Eggenstein-Leopoldshafen, Germany

* Author to whom any correspondence should be addressed.

E-mail: gerardo.sosa@kit.edu

Keywords: stretchable electronics, inkjet-printing, strain sensors, electrochromic devices

Supplementary material for this article is available [online](#)

Abstract

Herein, we present an approach that allows versatile combination of inkjet-printed electronics and stretchable substrates. For this, we created a hybrid platform made out of stretchable Ecoflex covalently bonded via silane monolayers to flexible polyethylene terephthalate islands interconnected by bridges. The islands served as platforms where conductive lines, capacitive sensors and electrochromic devices (ECDs) were fabricated by inkjet printing. The robustness of the approach is highlighted by the minor influence of strain on the conductivity of printed Ag electrodes, which changed the resistance only by 1.3% at an applied strain of 50%. Furthermore, we demonstrated capacitor sensors capable of responding to strain changing their capacitance from 0.2 to 1.6 pF. To further show the applicability of the approach for multilayer/multimaterial optoelectronic elements, we processed ECDs capable of displaying information on the stretchable platform. Thus, we demonstrate how this digital and additive concept can be applied for the scalable integration of printed optoelectronic devices onto stretchable systems without relying on lithographic processes.

1. Introduction

During the last decade, the field of flexible and stretchable electronics has paved the way to transform rigid optoelectronic elements into tailored functional elastic systems [1–3]. The latest research has demonstrated devices exhibiting sensing, optoelectronic, or energy harvesting capabilities which are able to withstand large mechanical deformations and conform to curvilinear surfaces [4, 5]. These promising achievements are set to enable the next-generation of applications in human health monitoring [6, 7], electronic implants [8], wearables [9, 10], e-skins [11], and smart textiles [12].

Ideally, all components in stretchable electronic systems should entirely utilize intrinsically elastic materials to avoid mechanically induced degradation during operation. Examples of such materials are liquid metal alloys, conductive hydrogels,

semiconducting composites, or elastomeric substrate materials [13–17]. However, the fabrication of inherently stretchable electronic systems is hindered by the limited variety of functional materials simultaneously exhibiting great elasticity (i.e. low Young's modulus) and high-performance semiconducting, dielectric, or conductive properties [5]. For this reason, the typical approaches to fabricate stretchable electronic systems entail the integration of inelastic functional materials, devices, or layers onto stretchable substrates [3]. This has been shown in literature through several approaches such as the processing of devices onto prestretched substrates [2], the utilization of resilient geometric structures (e.g. horseshoe patterns) [18], or the fabrication of interconnected rigid islands onto which devices are fabricated [15, 19–23]. The latter presents the main advantage of protecting the functional devices from strain by the underlying rigid islands while the overall electronic

system retains stretchability due to the flexible interconnecting bridges. These interconnects are either fabricated in form of resilient geometric patterns or arched bridge-type structures. Devices utilizing these architectures have been reported to withstand large mechanical strain without plastic deformation or failure in applications such as complementary metal-oxide-semiconductor (CMOS) inverters and oscillators [21], organic light-emitting diode (OLED) displays [20], health-monitoring sensors [19], and integrated circuits [24]. Generally, the assembly of such complex multi-device stretchable electronic systems requires a combination of several fabrication steps such as lithography, vacuum deposition, transfer-printing, or pick-and-place approaches as well as the need of high processing temperature, sacrificial layers, or elaborated high-vacuum systems [20–22, 25, 26]. Despite the current demonstration of inspiring technological examples, such a complex process chain hinders the high-throughput production and facile utilization of stretchable substrates as universal electronic platforms beyond the laboratory scale.

The utilization of digital and additive printing techniques could offer alternative pathways to the fabrication of functional devices onto stretchable substrates. Techniques such as inkjet printing are established tools in the field of printed electronics for a large variety of solution-processable materials and optoelectronic device architectures [27–34]. Despite also allowing the low-temperature processing, scalability, cost efficiency, and freedom of design necessary in the majority of the envisioned stretchable electronics applications, it has mainly been utilized for the deposition of single layers, such as conductive traces in resilient geometric structures or on prestretched substrates [4, 35–37]. Therefore, it is favorable to develop approaches that allow the seamless transfer of established inkjet-printing processes developed for commonly used flexible substrates, such as polyethylene terephthalate (PET) or polyethylene naphthalate, to fabricate stretchable systems.

In this work, we present a versatile way of fabricating inkjet-printed devices such as strain sensors and electrochromic devices (ECDs) onto stretchable hybrid substrates utilizing rigid islands interconnected by flexible bridges. The functional substrate is based on the commercially available silicone material Ecoflex onto which a laser-cut PET foil is covalently bonded via self-assembled monolayers (SAMs) to form islands and bridge-type interconnects. The rigid PET islands are utilized as a platform onto which the digitally-printed devices are fabricated while the bridge structures grant the ability to connect multiple devices. First, we investigate the strength of the chemical bonding between PET and Ecoflex as a function of bonding temperature, time and pressure. Secondly, we show that the conductivity of inkjet-printed silver electrodes was unaffected by the strain applied on the substrate. Furthermore, we

fabricate novel capacitive strain sensors utilizing the change in the arched bridges height upon substrate stretching. Finally, we demonstrate the applicability of the substrates for the fabrication of an array of inkjet-printed ECDs.

2. Results and discussion

To create the hybrid substrate we combined a highly stretchable substrate made of Ecoflex with a flexible but non stretchable PET foil. For this process we investigated the two silanes (3-aminopropyl)triethoxysilane (APTES) and (3-glycidyloxypropyl)trimethoxysilan (GLYMO), whose chemical structure is represented in figure 1(a), to covalently bond both substrates. This type of silanes have been used in literature to form SAMs onto various substrates via the headgroup, while the functional endgroup is used to form covalent bonds with a second surface [38–40]. Reactive groups on the substrate surface are necessary for the formation of the SAM, in the case of PET we utilized a O_2 plasma treatment for 5 min to generate OH groups onto which the anchor groups of the silanes can bond. In the case of Ecoflex, we utilized existing non-crosslinked reactive groups, such as OH groups, on which GLYMO is able to bond to [41, 42]. For the chemical bonding used in this work, the primary amine group of APTES covering the PET substrate forms a covalent bond with the terminal carbon atom of the epoxy group of GLYMO (deposited on Ecoflex), while its carbon–oxide bonds breaks to form an hydroxy group [39, 43]. The schematic representation of the process as well as the silane chemical reaction are represented in figure 1(b).

In a first step, the formation of the silane-SAMs on both substrates was investigated by measuring the contact angle of water before and after deposition of the SAM as depicted in figure 1(c). The pristine substrates exhibit a contact angle of $110 \pm 3^\circ$ and $54 \pm 3^\circ$ for Ecoflex and PET, respectively. For PET, this value decreased significantly to $8.0 \pm 0.5^\circ$ after oxygen plasma treatment. After the deposition of the respective silanes the substrates exhibit contact angles around $62 \pm 2^\circ$ for PET and $69.75 \pm 5^\circ$ for Ecoflex. This change in contact angles suggests a successful deposition of the SAMs. We used the same process of deposition on glass as reference to check the measured contact angles. Furthermore, these values fit well into the range of contact angles reported in literature for the respective SAM [39, 44, 45]. The high hydrophobicity of Ecoflex hindered a homogeneous deposition of GLYMO. To improve SAM formation, rough features were introduced into the Ecoflex substrate by laser-engraving certain parts of the mold used to produce the substrate. The roughness in the Ecoflex-substrate suppressed the dewetting and thus allowed a controlled deposition of the silane solution (see figure S1(a) and movie S1 in the SI available online at stacks.iop.org/FPE/7/025007/mmedia).

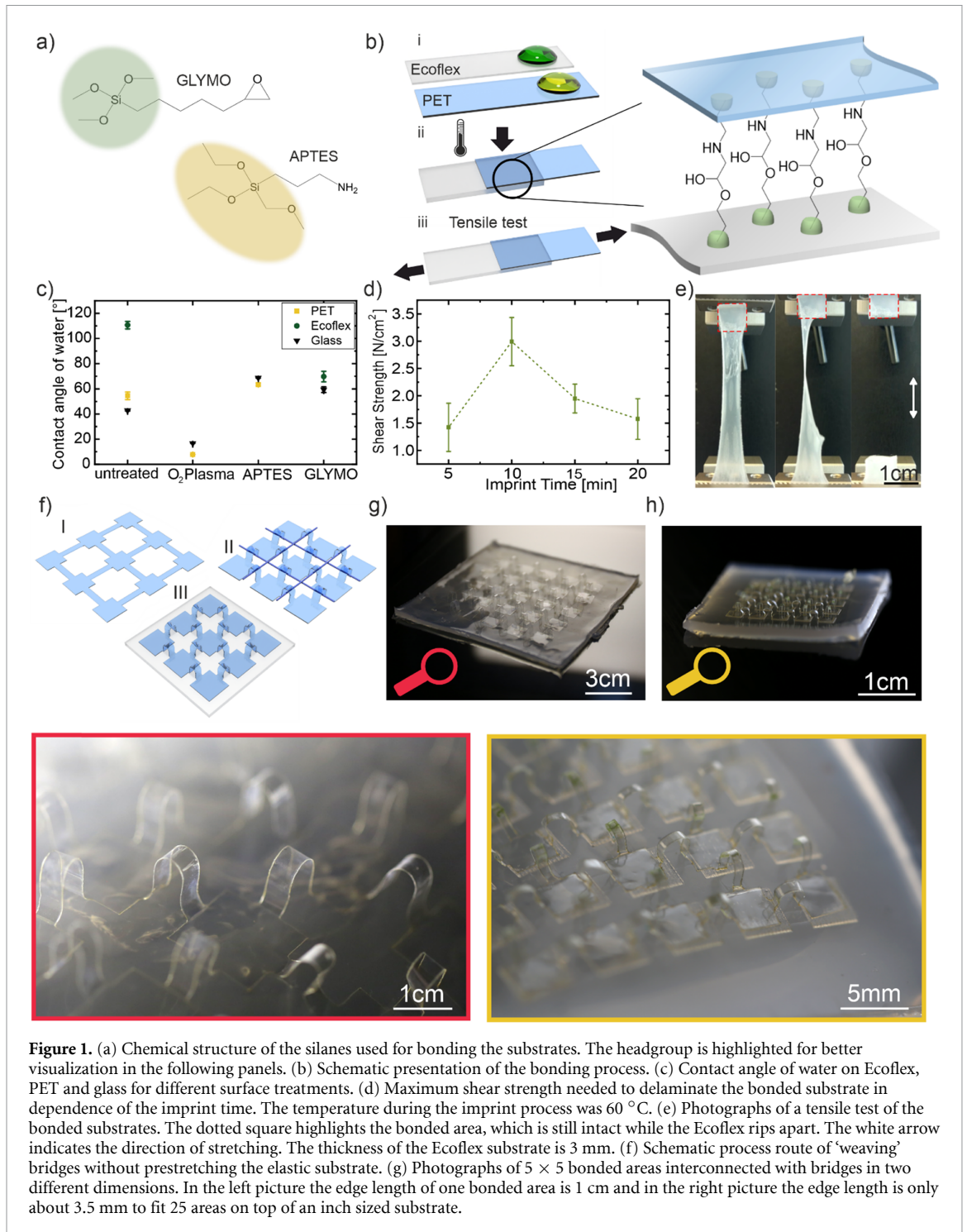


Figure 1. (a) Chemical structure of the silanes used for bonding the substrates. The headgroup is highlighted for better visualization in the following panels. (b) Schematic presentation of the bonding process. (c) Contact angle of water on Ecoflex, PET and glass for different surface treatments. (d) Maximum shear strength needed to delaminate the bonded substrate in dependence of the imprint time. The temperature during the imprint process was 60 °C. (e) Photographs of a tensile test of the bonded substrates. The dotted square highlights the bonded area, which is still intact while the Ecoflex rips apart. The white arrow indicates the direction of stretching. The thickness of the Ecoflex substrate is 3 mm. (f) Schematic process route of 'weaving' bridges without prestretching the elastic substrate. (g) Photographs of 5 × 5 bonded areas interconnected with bridges in two different dimensions. In the left picture the edge length of one bonded area is 1 cm and in the right picture the edge length is only about 3.5 mm to fit 25 areas on top of an inch sized substrate.

After depositing the silanes onto the substrates, we performed the bonding process by applying a temperature of 60 °C and pressure (5.5 bar) over time in an imprinter (figure 1(a(ii))). Figure 1(d) shows the maximal shear strength the bonded substrates were able to withstand as a function of imprinting time at a constant temperature of 60 °C. The presented value is an average over 4 different samples. The corresponding measurements and evaluation of a typical measurement can be found in figure S1(b) in the SI. Herein, the maximal shear strength corresponding to the failure point was used as the parameter

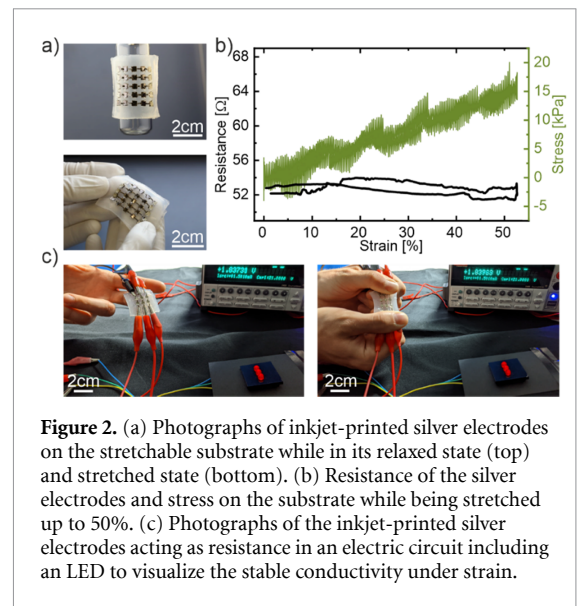
determining the quality of the bond between both materials (figure S1(c)). We observed that a maximum shear strength of $3.0 \pm 0.4 \text{ N cm}^{-2}$ is reached after 10 min imprint time. Additional experiments presented in figure S1(d) of the SI showed that extended periods of either temperature or pressure are detrimental to the bonding strength. The photographs in figure 1(e) and movie S2 in the SI, show that the failure point resides on the Ecoflex substrate and not at the interface of both materials, demonstrating the robustness of the developed hybrid substrate. For comparison, the stress-strain diagrams of

Ecoflex and of PET can be found in figure S1(e) in the supporting information.

The fabrication route to create the hybrid substrate comprising islands and bridges is schematically illustrated in figure 1(f). First, the PET foil was laser-cut in the desired pattern which would form the islands and bridge structures (I). Subsequently, the bridges are ‘weaved’ (II) with the help of a mask and thin rods. The PET substrate areas dedicated to the islands are located beneath the mask, while the bridges stay above. This makes sure the islands can easily be in contact to the Ecoflex substrate. After the bonding process, the rods are pulled out and the mask is lifted (III). This method prevents the whole composite from any prestretching and thus from undesired curling due to the mismatched mechanical properties of PET and Ecoflex.

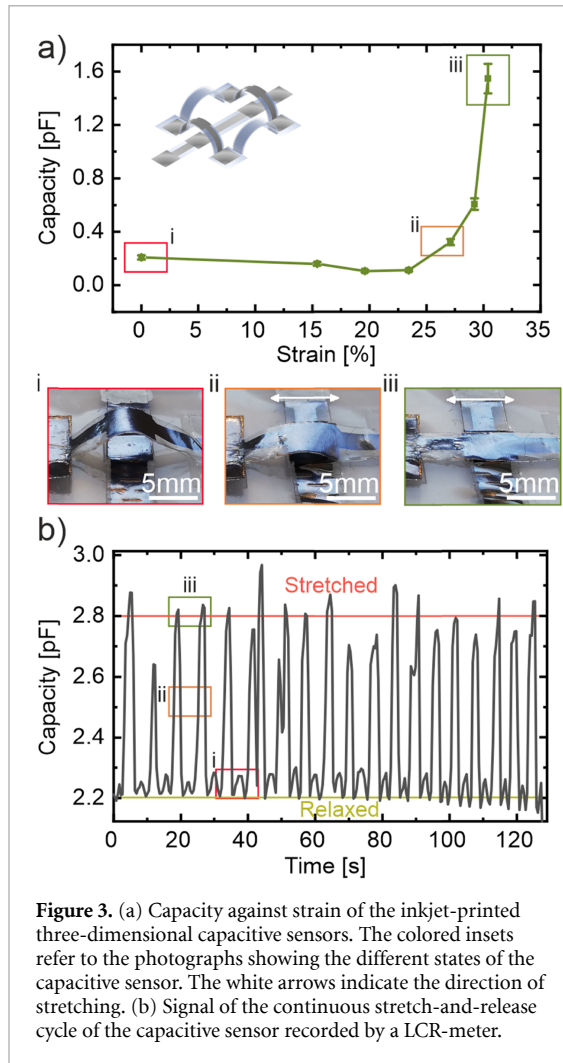
A detailed analysis of the bonding to prestretched Ecoflex substrates is presented in figure S2 in the SI. The curling effect occurring when prestretching the Ecoflex before bonding rules out proper use of the substrate for electronic devices. In our work, we utilized 12 μm thick PET foil to minimize any buckling or curling effects occurring from the rigidity of the flexible foil (SI, S2(c)). Figure 1(g) shows a hybrid substrate comprised of 25 islands connected by bridges fabricated through this method. The substrate has a total edge length of about 10 cm with 1 cm^2 islands connected by 14 mm long bridges. We demonstrate the miniaturization of the process by fabricating a hybrid substrate with a total edge length of 2.5 cm containing 25 islands with an area of 0.1225 cm^2 and bridges with a length of 5 mm (figure 1(h)). Magnified images of the two differently sized hybrid, stretchable platforms are shown at the bottom of figure 1. By performing a tensile test on the Ecoflex substrate with bonded PET islands interconnected by bridges one can see in figure S3 in the SI, that the Ecoflex stretches with minor mechanical resistance up to the maximum strain of the whole substrate defined by design ($\sim 50\%$). Beyond this strain, the mechanical resistance of the PET foil dominates until the bridges or the islands start breaking at around 60%. Because of its isotropic design in perpendicular directions, the stretching behavior should be the same in these directions.

To demonstrate the applicability of the developed approach for printed electronics, we firstly investigated the influence of strain caused on conductive silver electrodes deposited on the hybrid platform. Figure 2(a) shows five conductive paths comprised of five islands connected by arched bridges. These electrodes were inkjet-printed and annealed on top of the PET before the bonding process. The resistance of the electrodes vs applied strain can be seen in figure 2(b). The resistance fluctuates about 1.3% around the mean value of 52.8 Ω while the device is stretched up to $\sim 50\%$ of its initial length and released again. The maximum extension of the



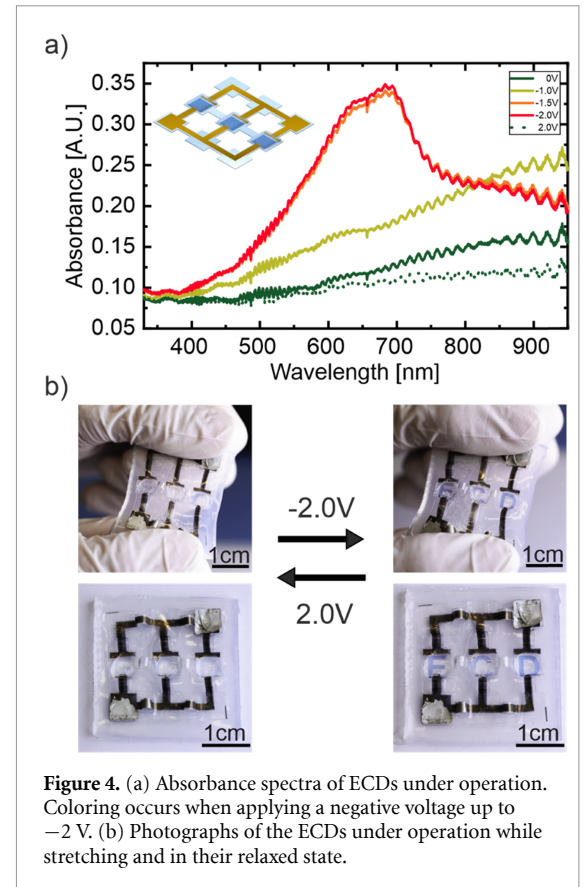
substrate was determined by the length of the bridges. For a better visualization of the stability of the electrodes we attached three commercial light-emitting diodes (LED) to three individual conductive paths (figure 2(c)). The applied voltage at constant current only changed by a ~ 4 mV during stretching and no flickering of the LEDs was observed (see movie S3 in the supporting information). Additionally, we measured the change in resistance over more than 7500 cycles of continuous stretch and release (figure S4, SI). One cycle of stretching to 50% strain and releasing again took 1.5 s. We determined a standard derivation of only 1.4% of the starting value across all cycles. This result highlights that electronics processed on top of the stretchable island-bridge platforms would be marginally affected by applied strain.

The stability shown by the electrodes enabled us to develop capacitive sensors by introducing a second electrode in the perpendicular direction underneath the bridges. Here the change in capacitance measured via impedance spectroscopy is correlated to the applied strain on the substrate which reduces the distance between the electrodes. The nominal area of the capacitor (25 mm^2) is determined by the overlapping of the Ag lines, however the effective capacitance also includes the contribution from the nearby electrode buzz lines. A schematic representation of this device capable of detecting the elongation state (i.e. strain) of the substrate is shown in the inset of figure 3(a). In the relaxed state (i), the sensor shows a capacitance of ~ 0.2 pF ($\pm 7.9\%$), which increases up to 1.6 pF ($\pm 7.1\%$) (iii) when the substrate is stretched to the maximum allowed length determined by the bridge structures (i.e. 30%). Such sensor could be used for determining the elongation state of a stretchable device. Photographs of different states of the capacitor can be found at the bottom of figure 3(a) with their corresponding capacitance value marked in the graph. A snapshot of about 20 stretch and release cycles can be seen in figure 3(b). Herein, the strain



sensor shows a relative change in capacitance $\Delta C/C$ of around 27% at a strain of 30%, which is comparable to capacitive strain sensors in literature [46–48].

Finally, we demonstrate the applicability of the stretchable hybrid platform for multi-material multi-device integration by fabricating ECDs on top of the rigid islands. The ECD architecture (inset figure 4(a)) is comprised of poly(3,4-ethylenedioxythiophene) polystyrene sulfonate (PEDOT:PSS) as electrochromic material connected by gold electrodes and covered by a gelatin-based electrolyte. The graph in figure 4(a) shows the change in absorbance of a reference ECD on top of 12 μm PET foil by applying a voltage of up to -2 V indicating a color change from transparent to dark blue. The wavy pattern in the absorbance spectra originates from optical interference in the thin substrate foil. By applying a voltage of -2 V at the electrode connected to the electrochromic material, the devices exhibit a contrast of $31.8 \pm 3.8\%$, a coloration efficiency of $156 \pm 74\text{ cm}^2\text{ C}^{-1}$ and switching times of $0.985 \pm 0.104\text{ s}$ (coloring) and $1.05 \pm 0.18\text{ s}$ (bleaching). These figures of merit fit well to our previously reported results for the same material system [49]. Photographs of the device under operations while stretched or relaxed can be



found in figure 4(b). Herein, we printed letters forming the abbreviation ECD for ECDs as the active layer on a stretchable substrate with nine islands with an area of 0.64 cm^2 of interconnected by 8 mm long bridges. No noticeable change in the color of the device was observed while stretching the substrate, suggesting that the active materials did not undergo mechanically induced degradation. A more in-depth look of the performance of electrical devices under repeated strain will be part of future work. Based on the presented results, we assume that the stretchable, hybrid platform is suited for a variety of complex multilayer devices and designs.

3. Conclusion

In summary, we demonstrated the integration of inkjet-printed conductive lines, sensors and ECDs onto stretchable substrates. The devices were processed onto PET foils which can be covalently bonded by SAMs to the stretchable substrate forming a robust hybrid platform where mechanical stress upon the functional devices is minimized. We showed that the resistance of printed Ag electrodes was unaffected by stretching the platform and demonstrated a capacitive sensor able to determine the state of stretching of the platform. Finally, the fabrication of ECDs onto the stretchable platform indicate the compatibility of the approach with the manufacturing of multi-material and multi-device stretchable systems. Thus,

we demonstrated that the presented digital and additive concept can be applied for the scalable integration of printed optoelectronic devices onto stretchable systems without relying on commonly used lithographic processes.

4. Methods

4.1. Materials

APTES (Acros Organics, 99%), GLYMO (Acros Organics, 99%), ethanol ($\geq 99.9\%$ (GC)), Ag-Ink (Silver dispersion, nanoparticle, 30–35 wt%), sodium chloride (NaCl, 99%), gelatin (from porcine skin) and glycerol (99%) were purchased from Sigma Aldrich. Ecoflex (00–20) and SOLARIS were obtained from KauPo Plankenhorn e.K. PEDOT:PSS(FHC Solar) was purchased from Heraeus. The gold ink (DryCure Au-J, 1010B) was obtained from C-Ink. The materials were used as received. The PET was purchased from Pütz GmbH + Co. Folien KG.

4.2. Bonding

The PET foil was cleaned in isopropanol in an ultrasonication bath for 10 min. The Ecoflex and SOLARIS substrates were produced by mixing its liquid components, pouring it in a mold and baking it at 90 °C for 30 min in a vacuum oven. APTES and GLYMO were dissolved in ethanol (5 vol%). These solutions were applied by dropcasting for 5 min on the substrate. Subsequently, the substrates were rinsed with isopropanol and dried with nitrogen. The foils and the ecoflex substrates were bonded in a nanoimprinter (CNI v1.0, NIL Technology ApS).

4.3. Fabrication of the electrodes and capacitors

The silver electrode structures were deposited on the precleaned PET foil by inkjet printing. Silver ink was printed with a 10 pl DMC11610 Fujifilm Dimatix cartridge with an individual waveform on a Pixdro LP50 (Meyer Burger). The dried layers were sintered at 120 °C for 30 min and encapsulated with scotch tape. After encapsulation the foil was lasercut with a Trotec Laserman Speedy 300.

4.4. Fabrication of the electrochromic devices (ECDs)

The fabrication route is the same to our previous publication [49]. The gold electrodes and the PEDOT layer were printed with a 10 pl cartridge on a Pixdro LP50 with an individual waveform. Gelatin was dissolved in deionized water at a concentration of 133 g l⁻¹ together with 0.15 mol l⁻¹ of sodium chloride at 50 °C on a hotplate serving as the electrolyte. When the gelatin was fully dissolved, glycerol was added to achieve a 6:1 weight ratio of glycerol to gelatin (798 g l⁻¹ glycerol). The solution was stirred for 30 min on a hotplate at 50 °C to achieve a homogeneous mixture and applied on top of the electrochromic layer afterwards.

4.5. Characterization methods

To ensure reliable contact between the devices and the clamps used to connect the measurement systems, silver paste was applied on the contact area beforehand. A PGSTAT128N (AutoLab) was used to measure the I–V characteristics of the EC devices. For the UV–visible spectroscopy measurements an AvaSpec-ULS3648 (Avantes) and a light source ranging from 300 to 1100 nm were used. The electrical properties of the electrodes and capacitors were measured with the PGSTAT128N and a LCR-meter. The measurements of the contact angles were conducted with a Krüss DSA-100 measurement setup. Layer thicknesses were measured with a profilometer from Dektak and their morphologies were investigated by microscopy with a Nikon Eclipse 80i. Tensile tests were done with an Alluris FMT-310BU tensile tests machine, where the force was measured with a FMT-310FUC5 50N (precision of 0.01 N) unit at a speed of 10 mm min⁻¹.

Data availability statement

The data that support the findings of this study are available upon reasonable request from the authors.

Acknowledgments

This project was partially supported by the German Federal Ministry of Education and Research (BMBF) through Grant FKZ: 03X5526, as well as the Deutsche Forschungsgemeinschaft (DFG) through Grant HE 7056/4-1. The authors thank Kai Xia for helping design the 3D renders.

ORCID iD

Gerardo Hernandez-Sosa  <https://orcid.org/0000-0002-2871-6401>

References

- [1] Lee H, Jiang Z, Yokota T, Fukuda K, Park S and Someya T 2021 Stretchable organic optoelectronic devices: design of materials, structures, and applications *Mater. Sci. Eng. R* **146** 100631
- [2] Qi D, Zhang K, Tian G, Jiang B and Huang Y 2021 Stretchable electronics based on PDMS substrates *Adv. Mater.* **33** 2003155
- [3] Wu W 2019 Stretchable electronics: functional materials, fabrication strategies and applications *Sci. Technol. Adv. Mater.* **20** 187–224
- [4] Fernandes D F, Majidi C and Tavakoli M 2019 Digitally printed stretchable electronics: a review *J. Mater. Chem. C* **7** 14035–68
- [5] Kim D C, Shim H J, Lee W, Koo J H and Kim D 2020 Material-based approaches for the fabrication of stretchable electronics *Adv. Mater.* **32** 1902743
- [6] Gao Q, Zhang J, Xie Z, Omisore O, Zhang J, Wang L and Li H 2019 Highly stretchable sensors for wearable biomedical applications *J. Mater. Sci.* **54** 5187–223
- [7] Liu Y, Wang H, Zhao W, Zhang M, Qin H and Xie Y 2018 Flexible, stretchable sensors for wearable health monitoring:

- sensing mechanisms, materials, fabrication strategies and features *Sensors* **18** 645
- [8] Xu L *et al* 2014 3D multifunctional integumentary membranes for spatiotemporal cardiac measurements and stimulation across the entire epicardium *Nat. Commun.* **5** 3329
- [9] Trung T Q, Ramasundaram S, Hwang B U and Lee N E 2016 An all-elastomeric transparent and stretchable temperature sensor for body-attachable wearable electronics *Adv. Mater.* **28** 502–9
- [10] Song W, Yoo S, Song G, Lee S, Kong M, Rim J, Jeong U and Park S 2019 Recent progress in stretchable batteries for wearable electronics *Batteries Supercaps* **2** 181–99
- [11] Yang J C, Mun J, Kwon S Y, Park S, Bao Z and Park S 2019 Electronic skin: recent progress and future prospects for skin-attachable devices for health monitoring, robotics, and prosthetics *Adv. Mater.* **31** 1904765
- [12] Chen G, Li Y, Bick M and Chen J 2020 Smart textiles for electricity generation *Chem. Rev.* **120** 3668–720
- [13] Jo Y J, Ok J, Kim S Y and Kim T 2021 Stretchable and soft organic–ionic devices for body-integrated electronic systems *Adv. Mater. Technol.* **7** 2001273
- [14] Held M, Pichler A, Chabeda J, Lam N, Hindenberg P, Romero-Nieto C and Hernandez-Sosa G 2021 Soft electronic platforms combining elastomeric stretchability and biodegradability *Adv. Sustain. Syst.* **6** 2100035
- [15] Silva C A, Lv J, Yin L, Jeerapan I, Innocenzi G, Soto F, Ha Y G and Wang J 2020 Liquid metal based island-bridge architectures for all printed stretchable electrochemical devices *Adv. Funct. Mater.* **30** 1–10
- [16] Zhao X, Chen F, Li Y, Lu H, Zhang N and Ma M 2018 Bioinspired ultra-stretchable and anti-freezing conductive hydrogel fibers with ordered and reversible polymer chain alignment *Nat. Commun.* **9** 3579
- [17] Khan A, Kisannagar R R, Gouda C, Gupta D and Lin H C 2020 Highly stretchable supramolecular conductive self-healable gels for injectable adhesive and flexible sensor applications *J. Mater. Chem. A* **8** 19954–64
- [18] Amjadi M, Yoon Y J and Park I 2015 Ultra-stretchable and skin-mountable strain sensors using carbon nanotubes–Ecoflex nanocomposites *Nanotechnology* **26** 375501
- [19] Mohan A M V, Kim N H, Gu Y, Bandodkar A J, You J M, Kumar R, Kurniawan J F, Xu S and Wang J 2017 Merging of thin- and thick-film fabrication technologies: toward soft stretchable ‘island–bridge’ devices *Adv. Mater. Technol.* **2** 1–7
- [20] Park S I *et al* 2009 Printed assemblies of inorganic light-emitting diodes for deformable and semitransparent displays *Science* **325** 977–81
- [21] Kim D-H, Song J, Choi W M, Kim H-S, Kim R-H, Liu Z, Huang Y Y, Hwang K-C, Zhang Y-W and Rogers J A 2008 Materials and noncoplanar mesh designs for integrated circuits with linear elastic responses to extreme mechanical deformations *Proc. Natl Acad. Sci. USA* **105** 18675–80
- [22] Cheng X, Zhang F, Bo R, Shen Z, Pang W, Jin T, Song H, Xue Z and Zhang Y 2021 An anti-fatigue design strategy for 3D ribbon-shaped flexible electronics *Adv. Mater.* **33** 2102684
- [23] Xue Z, Song H, Rogers J A, Zhang Y and Huang Y 2020 Mechanically-guided structural designs in stretchable inorganic electronics *Adv. Mater.* **32** 1902254
- [24] Huang Z *et al* 2018 Three-dimensional integrated stretchable electronics *Nat. Electron.* **1** 473–80
- [25] Sun Y, Choi W M, Jiang H, Huang Y Y and Rogers J A 2006 Controlled buckling of semiconductor nanoribbons for stretchable electronics *Nat. Nanotechnol.* **1** 201–7
- [26] Ko H C *et al* 2008 A hemispherical electronic eye camera based on compressible silicon optoelectronics *Nature* **454** 748–53
- [27] Kwon J, Baek S, Lee Y, Tokito S and Jung S 2021 Layout-to-bitmap conversion and design rules for inkjet-printed large-scale integrated circuits *Langmuir* **37** 10692–701
- [28] Baek S *et al* 2022 Spatiotemporal measurement of arterial pulse waves enabled by wearable active-matrix pressure sensor arrays *ACS Nano* **16** 368–77
- [29] Zhan Z, An J, Wei Y, Tran V T and Du H 2017 Inkjet-printed optoelectronics *Nanoscale* **9** 965–93
- [30] Strobel N *et al* 2020 Color-selective printed organic photodiodes for filterless multichannel visible light communication *Adv. Mater.* **32** 1908258
- [31] Schliske S, Raths S, Ruiz-Preciado L A, Lemmer U, Exner K and Hernandez-Sosa G 2021 Surface energy patterning for ink-independent process optimization of inkjet-printed electronics *Flex. Print. Electron.* **6** 015002
- [32] Pietsch M, Rödlmeier T, Schliske S, Zimmermann J, Romero-Nieto C and Hernandez-Sosa G 2019 Inkjet-printed polymer-based electrochromic and electrofluorochromic dual-mode displays *J. Mater. Chem. C* **7** 7121–7
- [33] Strobel N, Seiberlich M, Rödlmeier T, Lemmer U and Hernandez-Sosa G 2018 Non-fullerene-based printed organic photodiodes with high responsivity and megahertz detection speed *ACS Appl. Mater. Interfaces* **10** 42733–9
- [34] Zimmermann J, Schliske S, Held M, Tisserant J-N, Porcarelli L, Sanchez-Sanchez A, Mecerreyes D and Hernandez-Sosa G 2019 Ultrathin fully printed light-emitting electrochemical cells with arbitrary designs on biocompatible substrates *Adv. Mater. Technol.* **4** 1800641
- [35] Huang Q and Zhu Y 2019 Printing conductive nanomaterials for flexible and stretchable electronics: a review of materials, processes, and applications *Adv. Mater. Technol.* **4** 1800546
- [36] Adly N, Weidlich S, Seyock S, Brings F, Yakushenko A, Offenhäusser A and Wolfrum B 2018 Printed microelectrode arrays on soft materials: from PDMS to hydrogels *npj Flex. Electron.* **2** 15
- [37] Hassan G, Bae J, Hassan A, Ali S, Lee C H and Choi Y 2018 Ink-jet printed stretchable strain sensor based on graphene/ZnO composite on micro-random ridged PDMS substrate *Composites A* **107** 519–28
- [38] Vlachopoulou M-E, Tserepi A, Pavli P, Argitis P, Sanopoulou M and Misiakos K 2009 A low temperature surface modification assisted method for bonding plastic substrates *J. Micromech. Microeng.* **19** 015007
- [39] Tang L and Lee N Y 2010 A facile route for irreversible bonding of plastic-PDMS hybrid microdevices at room temperature *Lab Chip* **10** 1274
- [40] Kim K, Park S W and Yang S S 2010 The optimization of PDMS-PMMA bonding process using silane primer *BioChip J.* **4** 148–54
- [41] Guillory X, Tessier A, Gratien G O, Weiss P, Collic-Jouault S, Dubreuil D, Lebreton J and Le Bideau J 2016 Glycidyl alkoxy silane reactivities towards simple nucleophiles in organic media for improved molecular structure definition in hybrid materials *RSC Adv.* **6** 74087–99
- [42] Nguyen T, Jung S H, Lee M S, Park T E, Ahn S K and Kang J H 2019 Robust chemical bonding of PMMA microfluidic devices to porous PETE membranes for reliable cytotoxicity testing of drugs *Lab Chip* **19** 3706–13
- [43] Kumar A, Sundararaghavan V and Browning A R 2014 Study of temperature dependence of thermal conductivity in cross-linked epoxies using molecular dynamics simulations with long range interactions *Modelling Simul. Mater. Sci. Eng.* **22** 025013
- [44] Siqueira Petri D F, Wenz G, Schunk P and Schimmel T 1999 An improved method for the assembly of amino-terminated monolayers on SiO₂ and the vapor deposition of gold layers *Langmuir* **15** 4520–3
- [45] Howarter J A and Youngblood J P 2006 Optimization of silica silanization by 3-aminopropyltriethoxysilane *Langmuir* **22** 11142–7
- [46] Dong T, Gu Y, Liu T and Pecht M 2021 Resistive and capacitive strain sensors based on customized compliant electrode: comparison and their wearable applications *Sens. Actuators A* **326** 112720
- [47] Mo F, Huang Y, Li Q, Wang Z, Jiang R, Gai W and Zhi C 2021 A highly stable and durable capacitive strain sensor

- based on dynamically super-tough hydro/organo-gels *Adv. Funct. Mater.* **31** 2010830
- [48] Deng C *et al* 2020 High-performance capacitive strain sensors with highly stretchable vertical graphene electrodes *J. Mater. Chem. C* **8** 5541–6
- [49] Pietsch M, Schliske S, Held M, Strobel N, Wiczorek A and Hernandez-Sosa G 2020 Biodegradable inkjet-printed electrochromic display for sustainable short-lifecycle electronics *J. Mater. Chem. C* **8** 16716–24